Corrosion Science 94 (2015) 156–164

Contents lists available at ScienceDirect

Corrosion Science

journal homepage: www.elsevier.com/locate/corsci

# A statistical study on the effect of annealing temperature on pitting corrosion resistance of 2205 duplex stainless steel

M. Gholami, M. Hoseinpoor, M.H. Moayed *

*Metallurgical and Materials Engineering Department, Faculty of Engineering, Ferdowsi University of Mashhad, Mashhad 91775-1111, Iran*

ARTICLE INFO

*Article history:*
Received 24 October 2014
Accepted 30 January 2015
Available online 7 February 2015

*Keywords:*
A. Stainless steel
B. Polarisation
C. Pitting corrosion

ABSTRACT

In present work, pitting potential and metastable pitting occurrence of the 2205 duplex stainless steel were studied by means of statistical approaches at different annealing temperatures ranging from 1050 °C to 1250 °C. Obtained results showed that pitting resistance is considerably reduced by annealing alloy at 1250 °C. The microstructure investigation revealed the presence of Cr and N rich precipitates such as chromium nitrides ($Cr_2N$) in ferrite phase after rapid cooling from higher annealing temperature. Therefore, presence of these precipitates can be the main result of preferential pitting occurring in ferrite phase and reduction in pitting resistance of the alloy.



## 1. Introduction

As known, the low corrosion rate of the stainless steels in aqueous environments arises from the existence of a thin passivating oxide film on their surfaces. However, this passivating film is susceptible to localized breakdown from stochastic sites in unknown time which can be resulted to accelerated dissolution of the underlying metal. Among localized corrosion processes, extensive studies have been devoted to the pitting corrosion by researchers due to complexity of this field. For instance, up to now several pitting initiation mechanisms have been reported by authors but still there is not a general agreement about this step of pitting corrosion [1–5]. In addition, it is obvious that the effect of the pit propagation step on the probability of stable pits forming cannot be rolled out [6–9].

Generally, pitting resistance of the stainless steels is determined by their pitting potential ($E_{pit}$) or critical pitting temperature (CPT) values [10–12]. In this manner, the stainless steels with higher values of the pitting potential or critical pitting temperature show the better resistance to pitting corrosion. The corresponding values can be determined by means of electrochemical methods which accelerate pitting corrosion [13–16]. Although, it is worth noting that the pitting potential is generally stochastic and it cannot be considered as a unique value [17–19]. In this way, several stochastic models have been presented in order to predict pitting corrosion [20–26]. Also, statistical approaches have been applied in pitting corrosion studies in order to clarify unpredictable nature of pitting corrosion [19,27–31]. For instance, distribution of the pitting potential value scan be recognized well by use of cumulative probability graphs [32]. The cumulative probability can be calculated as follows:

$$P(x) = \frac{n}{1+N} \tag{1}$$

where $N$ is the total number of repeated experiments, and $n$ is the number of samples that showed pitting in a specific potential range. So, the cumulative probability of the pitting potential can be calculated by considering $n$ as the order in ordered pitting potential values and $N$ as the total number of the experiments [19]. In addition, Galvele indicated that for a one dimensional pit a minimum product of the current density ($i$) and the pit radius ($r$) is required to sustain the pit growth [33]. Hence, the cumulative probability graphs of this value introduced as the pit stability product can be used as another valuable criterion to determine pitting resistance [32]. Meanwhile, the value of 0.3 A $m^{-1}$ is considered as the critical value of the pit stability product [34]. Moreover, cumulative probability graph of nucleation frequency of the metastable pitting has been used by researchers [32].

It is generally accepted that the pitting potential is dependent on the environmental parameters, alloy composition, scan rate, heat treatment, etc. [35–39]. For instance, effect of the annealing temperature on corrosion resistance of the austenitic–ferritic duplex stainless steels has been widely investigated by authors [40–44]. Duplex stainless steels owe their considerable corrosion resistance to alloying elements such as Cr, Mo and N. However, the corrosion resistance of these stainless steels is highly dependent to their microstructure which is affected by heat treatment.

* Corresponding author. Tel.: +98 5118763305; fax: +98 5118763301.
*E-mail address:* mhmoayed@um.ac.ir (M.H. Moayed).

http://dx.doi.org/10.1016/j.corsci.2015.01.054
0010-938X/

During the processing such as welding, this alloy exposes to high temperatures which causes the metallurgical changes. Perren et al. [42,43] investigated the corrosion resistance of super duplex stainless steels in chloride contacting environments through a micro-electrochemical method. According to their results, inappropriate heat treatment of super duplex stainless may cause the precipitation of undesired phases, which drastically decrease the corrosion resistance. Tan et al. [44] studied the effect of the annealing temperature on pitting corrosion of the super duplex stainless steel UNS S32750 and concluded that by increasing annealing temperature from 1030 °C to 1080 °C elevates the critical pitting temperature while further increasing of the annealing temperature to the 1200 °C decreases the critical pitting temperature. They attributed the aforementioned results to the variation of the pitting resistance equivalent number (PREN) of ferrite and austenite phase by annealing temperature. The PREN indicates the resistance of a corrosion resistant alloy to pitting in the presence of water, chlorides and oxygen or oxidant environment and it is defined by Eq. (2). This equation reveals that the pitting corrosion resistance strongly depends on the content of Cr, Mo and N in stainless steels [45].

$$\mathrm{PREN} = \mathrm{wt.\%Cr} + 3.3\ \mathrm{wt.\%Mo} + 16\ \mathrm{wt.\%N} \quad (2)$$

Deng et al. [46] investigated the effect of annealing treatment on microstructure evolution and the associated corrosion behavior of a super-duplex stainless steel. They showed that the corrosion behavior is dependent on the microstructure, namely the presence of secondary phases, elemental partitioning behavior (alters the PREN value) and volume fractions of ferrite and austenite phases. Moura et al. [41] studied the Influence of microstructure on the corrosion resistance of the duplex stainless steel UNS S31803. They reported that the creation of the secondary phases such as sigma and $Cr_2N$ have the main role on decreasing of the pitting resistance. Likewise, deterioration effect of the secondary phases on corrosion resistance of the duplex stainless steels has been reported by other researchers [40,47,48]. However, up to now it has not been perform any investigation about the effect of annealing temperature on duplex stainless steels pitting resistance through statistical approaches.

The main aim of this work is to investigate the effect of the annealing temperature on metastable pitting and pitting potential of the 2205 duplex stainless steel (DSS 2205) by combination of the electrochemical methods and statistical approaches. For this purpose, pitting potential of the DSS 2205 is estimated by potentiodynamic polarisation method while the metastable pitting is investigated by potentiostatic polarisation technique. In addition, microstructure of the samples before and after pitting measurement is studied through light optical microscopy (LOM) and scanning electron microscopy (SEM).

## 2. Experimental

### 2.1. Sample preparation and heat treatment

The work was performed on the rod samples of the DSS 2205 with the chemical composition illustrated in Table 1. The samples were solution treated at 1050 °C, 1150 °C and 1250 °C for 45 min and then water quenched to room temperature.

### 2.2. Microstructure characterization

The microstructure of the samples before and after pitting potential measurement tests characterized through light optical microscopy. In this process, the characterization preformed on mirror-like samples etched by two procedures. Some samples were etched by Glyceregia solution (10 ml glycerol + 40 ml HCl + 10 ml $HNO_3$) while others were electrochemically etched by 10 wt.% NaOH solution at the anodic potential of 5 V for 1 min. The NaOH solution reveals just the austenite and ferrite phases, while the Glyceregia solution is capable to reveal high Cr and N rich precipitates such as $Cr_2N$ precipitates beside austenite and ferrite phases. In addition, characterization of this precipitates was also performed by SEM–EDS technique. In this process, the sample heat treated at 1250 °C was etched with an electrolytic etching technique proposed by Ramirez et al. [49].

### 2.3. Electrochemical measurements

All electrochemical measurements were performed with Gill AC potentiostat (ACM instruments). The saturated calomel electrode (SCE) and a platinum foil used as the reference and counter electrode, respectively. Before each measurement, the samples were successively wet ground by SiC emery papers from 60 to 1200, rinsed with distilled water and dried by air. The tests solution was the 3.5 wt.% NaCl solution made up by distilled water and analytical grade reagents. In addition, before electrochemical measurements the open-circuit potential was measured for 30 min.

#### 2.3.1. Critical pitting temperature measurement

The critical pitting temperature of the samples was estimated by polarisation curves, started from 100 mV below open-circuit potential with the scan rate of 1 mV $s^{-1}$. In this procedure, samples with the surface area of about 4 $cm^2$ were used. In addition, the measurements were repeated 3 times for each sample.

#### 2.3.2. Pitting potential measurement

The pitting potential of the samples were estimated at the temperature of 65 °C. For this purpose, the samples with the surface area of the 1 $cm^2$ were polarised dynamically from 100 mV below open circuit potential with the scan rate of 1 mV $s^{-1}$. The potential at which a significant increase in current density observed was considered as the pitting potential. The measurements were repeated 15 times for each sample.

#### 2.3.3. Metastable pitting measurement

Metastable pitting transients of the samples were recorded by potentiostatic polarisation method by the reading rate of 50 measurements per second. The measurements were performed at 43 °C and 65 °C by applying the anodic potential of the 800 and 80 mV/SCE, respectively. In addition, in order to reduce the overlap events, the samples with the surface area of about 0.2 $cm^2$ were used. The measurements were repeated 3 times for each sample.

**Table 1**
Chemical composition of the used DSS 2205 alloy (wt.%).

| Sample | C | Cr | Ni | Mo | S | P | Mn | Si | N | Other | Fe |
|---|---|---|---|---|---|---|---|---|---|---|---|
| DSS2205 | 0.03 | 21.61 | 5.31 | 3.07 | 0.0007 | 0.022 | 0.97 | 0.74 | 0.3 | <0.5 | Bal |

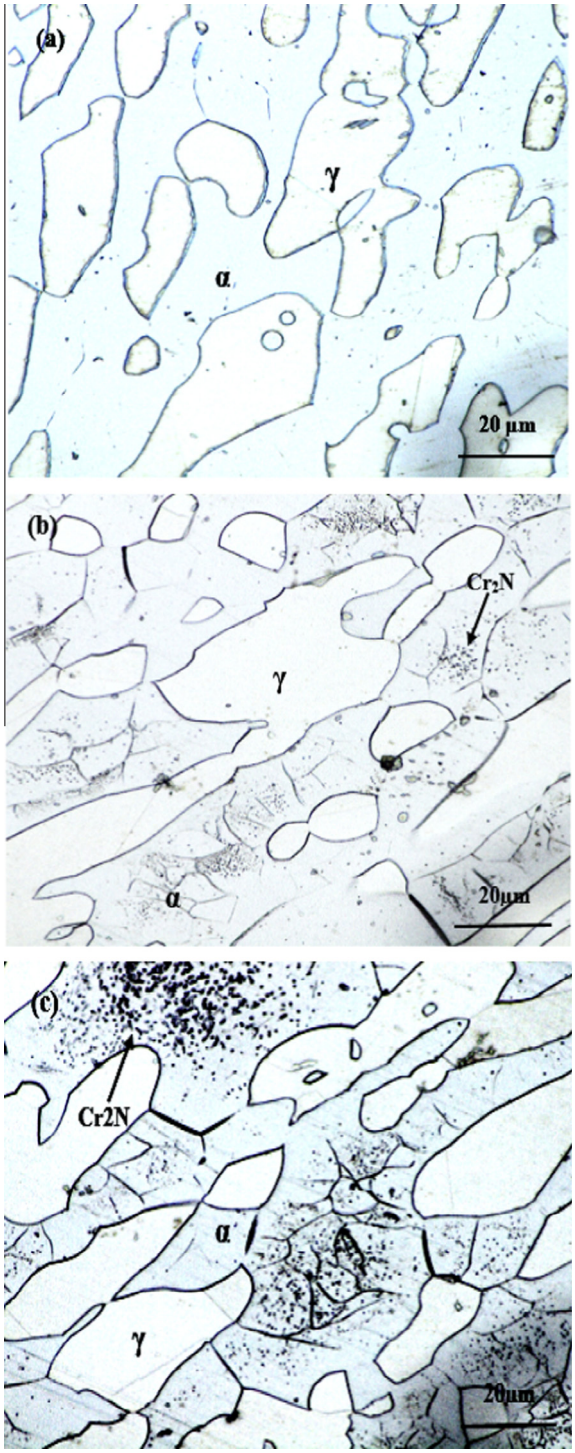


**Fig. 1.** Optical micrographs of the sample etched by Glycergia solution after heat treating at (a) 1050 °C, (b) 1150 °C, and (c) 1250 °C.

## 3. Experimental results

### 3.1. Microstructure characterization

Fig. 1 illustrates the microstructure of the samples annealed at different temperatures prior to pitting measurement obtained by etching at Glycergia solution. Etching by aforementioned solution cause to staining the ferrite phase and makes it to be appeared as the darker phase. According to Fig. 1, it is obvious that there is a direct link between annealing temperatures and the volume fraction of the ferrite phase. The plot of ferrite volume fraction versus solution annealing temperature are shown in Fig. 2. The volume fraction of ferrite for solution annealed at 1050 °C is 42% and increases to 52% and 69% for sample solution annealed at 1150 °C and 1250 °C respectively. This phenomenon can be appropriately described by means of phase transformation diagrams [50]. In addition, comparing the microstructures reveal that some black needles have been appeared in the center of ferrite phase (far from the ferrite/austenite interface) on the samples heat treated at 1150 °C and 1250 °C. The SEM image of this phase is shown in Fig. 3a. The analysis of the composition of the black needles by energy dispersive spectroscopy (EDS) connected to a field emission secondary electron microscope (FE-SEM) was shown in Fig. 3b and c. This figure demonstrates that the black needles is contained of high amounts of Cr and Ni elements. According to Garfias-Mesias et al. [38] the level of nitrogen presented in the ferrite phase is being assumed to be around 0.05% saturation with the rest partitioned to the austenite phase. So, during rapid quenching from high annealing temperatures, nitrogen close to the phase boundaries diffuses into adjacent austenite phase while presence of a high dislocation density at the ferrite sub-grain boundaries hamper diffusion of the remained nitrogen. As a result, the level of the nitrogen presented in the center of the ferrite phase is being super saturated and the chromium nitrides are precipitated as secondary phases. The only phase that is reported to be precipitated during Non-isothermal treatment is the chromium nitride phase (called quenched-in nitrides) [41,49]. Therefore, according to annealing temperatures and quenching procedure, the mentioned black needles could be corresponded to chromium nitrides precipitates. The similar microstructure has been also reported for other duplex stainless steels rapid quenched from high annealing temperatures [43].

### 3.2. Critical pitting temperature measurement

As known, the critical pitting temperature is the lowest temperature at which a sudden drop in breakdown potential from the transpassive range to the pitting range is observed. The typical potentiodynamic polarisation experiments at various temperatures for solution annealed samples are illustrated in Fig. 4. The critical pitting temperature values for heat treated samples obtained by polarisation curves, the samples heat treated at 1050 °C and 1150 °C have the same critical pitting temperature range (55–60 °C), while the sample heat treated at 1250 °C possess

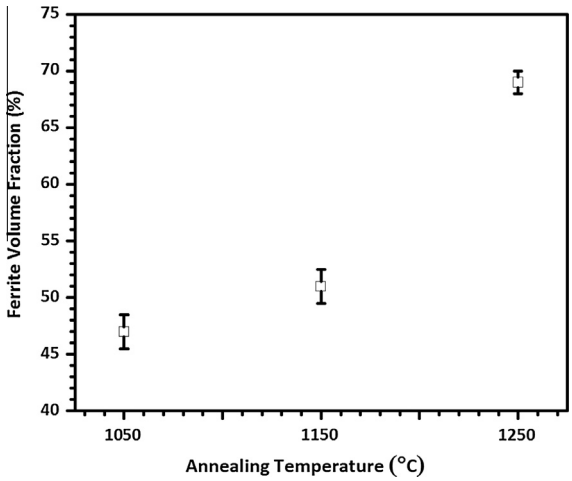


**Fig. 2.** The plot of ferrite phase fraction of alloy versus solution annealing temperature.

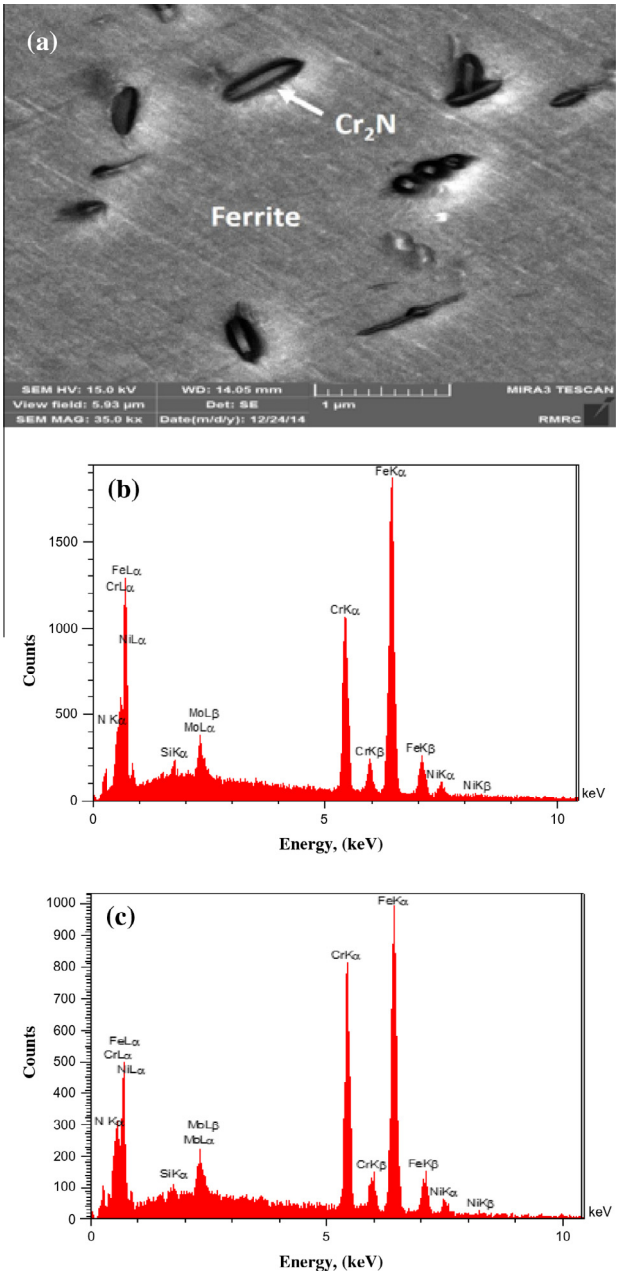


**Fig. 3.** (a) The FE-SEM image of sample showing the chromium nitride phase in ferrite matrix, (b) EDS spectrum of sample matrix, and (c) EDS spectrum of secondary phases (chromium nitride).

lower critical pitting temperature values (45–50 °C). Consequently, the pitting resistance of the DSS 2205 is diminished by elevating annealing temperature to 1250 °C. Moreover, the obtained results are used for further studies on pitting resistance measurement of the heat treated samples.

### 3.3. Pitting potential measurement

The pitting potential of the samples were determined at the temperature of 65 °C which was higher than the CPT value for applied samples. Fig. 5 presents the typical polarisation curves of the samples at the temperature of 65 °C with the applied criterion to determine pitting potential. It can be seen that the samples are at the passive state and the corrosion potential of the samples is at the range of -200 mV/SCE to −100 mV/SCE. Furthermore, Fig. 5 indicates that the passivity current density increases slightly with increasing heat treating temperature. Fig. 6 shows the cumulative distribution of the pitting potentials of the heat treated samples after 15 times repetition of the measurements at the temperature of 65 °C. Comparing the median values of pitting probability reveals that the samples heat treated at different temperatures have the pitting potential values in the order of

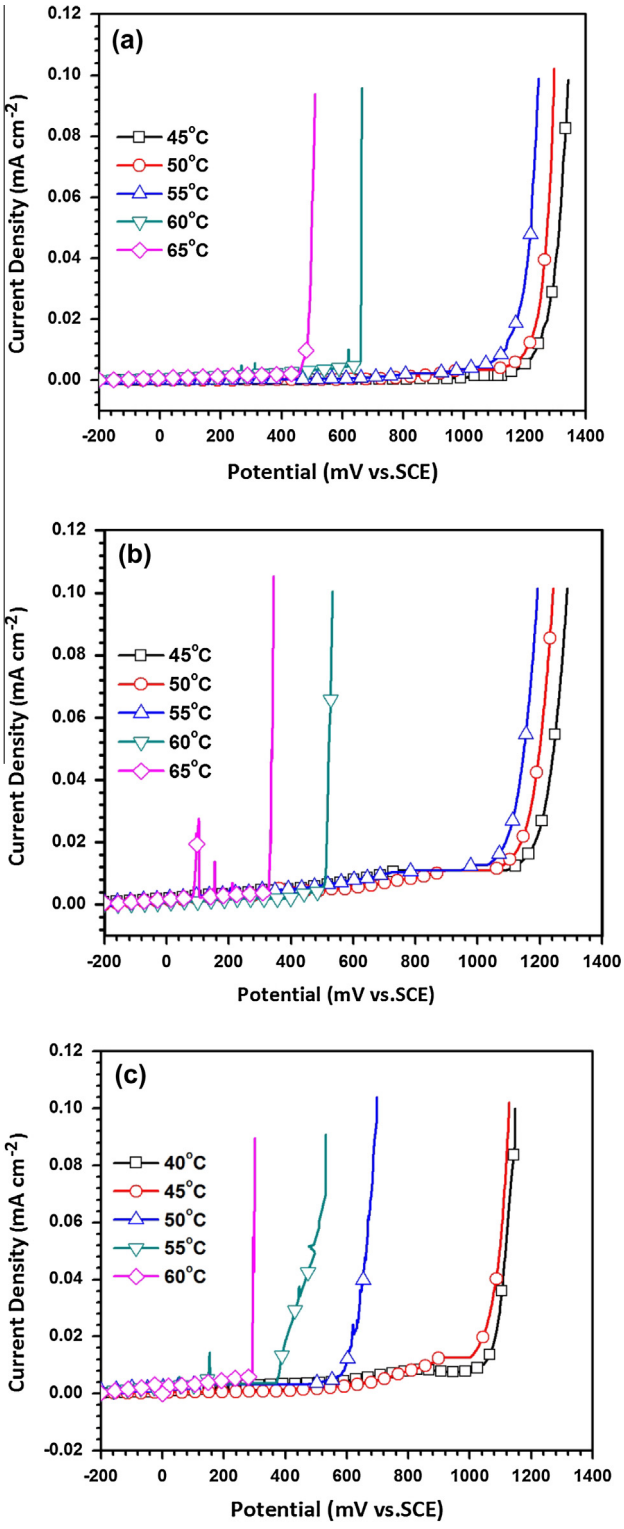


**Fig. 4.** Potentiodynamic polarisation curves of samples annealed at (a) 1050 °C, (b) 1150 °C, and (c) 1250 °C at various temperatures.

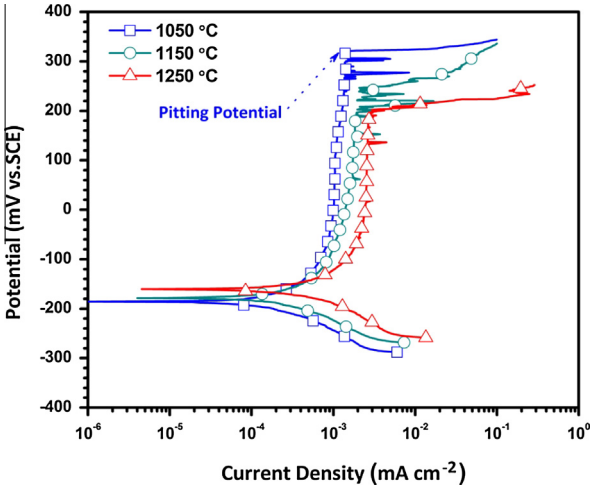


**Fig. 5.** Typical polarisation curves of the samples heat treated at different annealing temperatures with applied criterion to determine pitting potential.

1050 °C > 1150 °C > 1250 °C. Therefore, both pitting potential and critical pitting temperature values confirm reducing pitting resistance of the DSS 2205 by heat treating at 1250 °C. Furthermore, based in Fig. 6, the stochastic nature of the pitting corrosion can be recognized well.

After pitting potential measurement, the position of the formed pit was also investigated. The investigation was conducted in NaOH solution to avoid dissolving precipitates and consider them as formed pit incorrectly. Fig. 7 illustrates the position of the formed pit on the samples heat treated at different temperature. Similarly, the electrochemically etching of the samples by NaOH solution stains the ferrite phase and it appears as the darker phase. According to Fig. 7, stable pits are formed in austenite phase on the samples heat treated at 1050 °C. However, the ferrite phase is the main position of the stable pits for the samples heat treated at 1150 °C and 1250 °C. The lower PREN value of the ferrite phase for the samples heat treated at 1150 °C and 1250 °C is the responsible of the preferential pitting occurring in this phase [44,46].

### 3.4. Metastable pitting measurement

Metastable pits are pits with limited lifetime on the order of seconds or less [51]. So, as the metastable pits have a negligible

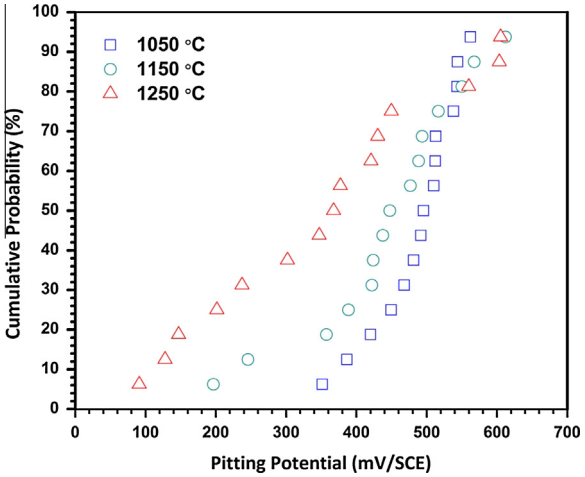


**Fig. 6.** Cumulative distribution of the pitting potential of the samples heat treated at different annealing temperatures.

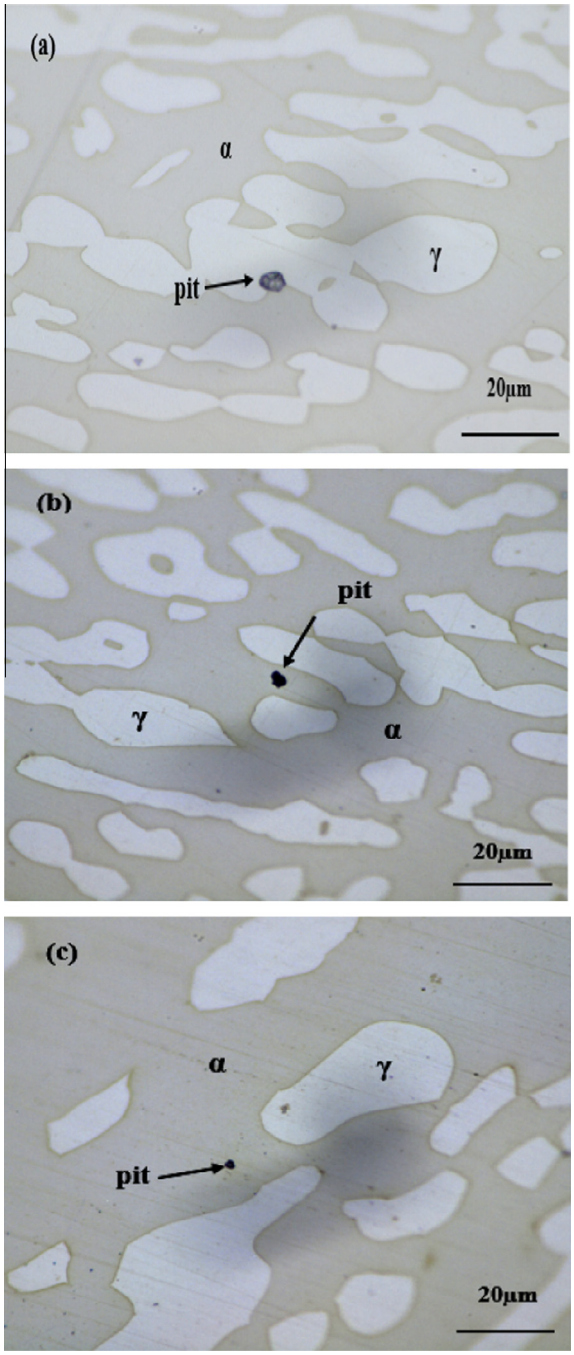


**Fig. 7.** Optical micrographs of the formed pits on the sample heat treated at (a) 1050 °C, (b) 1150 °C, and (c) 1250 °C after pitting potential measurements.

growth time duration, they are mainly associated with the pitting initiation step. However, there is a direct relation between stable pitting and metastable pitting. In this way, the samples with higher metastable pitting events ($\lambda$) are more susceptible to pitting corrosion due to having more susceptible sites on their surface. Similarly, the probability of forming stable pits increases by increasing metastable pits stability product ($i.r$). The mentioned values can be determined through potentiostatic polarisation method. The purpose of this experiment was the comparison of metastable pitting of alloy solution annealed at various temperatures and the evaluation of the effect of potential and temperature on pitting corrosion is not the purpose of this study. Potentiostatic polarisation measurements were performed at two

entirely different conditions. First, the polarisation was conducted at a temperature above the CPT (65 °C) at 80 mV/SCE. Figs. 8 shows the typical potentiostatic polarisation curves in this condition. Then the measurement was performed by applying the anodic potential of 800 mV/SCE at the temperature below the CPT (43 °C) (shown in Fig. 9). Selection of a different potential was in order to observe high enough number of current spike sufficient for the purpose of stochastic evaluation and comparison of the results obtained for various samples. The aforementioned conditions were selected to investigate the effect of both temperature and applying potential on metastable pitting.

Fig. 10 presents the average of metastable pits nucleation frequency $\lambda$ ($cm^{-2}\ s^{-1}$) for heat treated samples at the anodic potential of 80 and 800 mV/SCE for the temperature of 65 °C and 43 °C, respectively. The $\lambda$ values were calculated by counting the numbers of events every 50 s. As it can be seen, at the beginning of

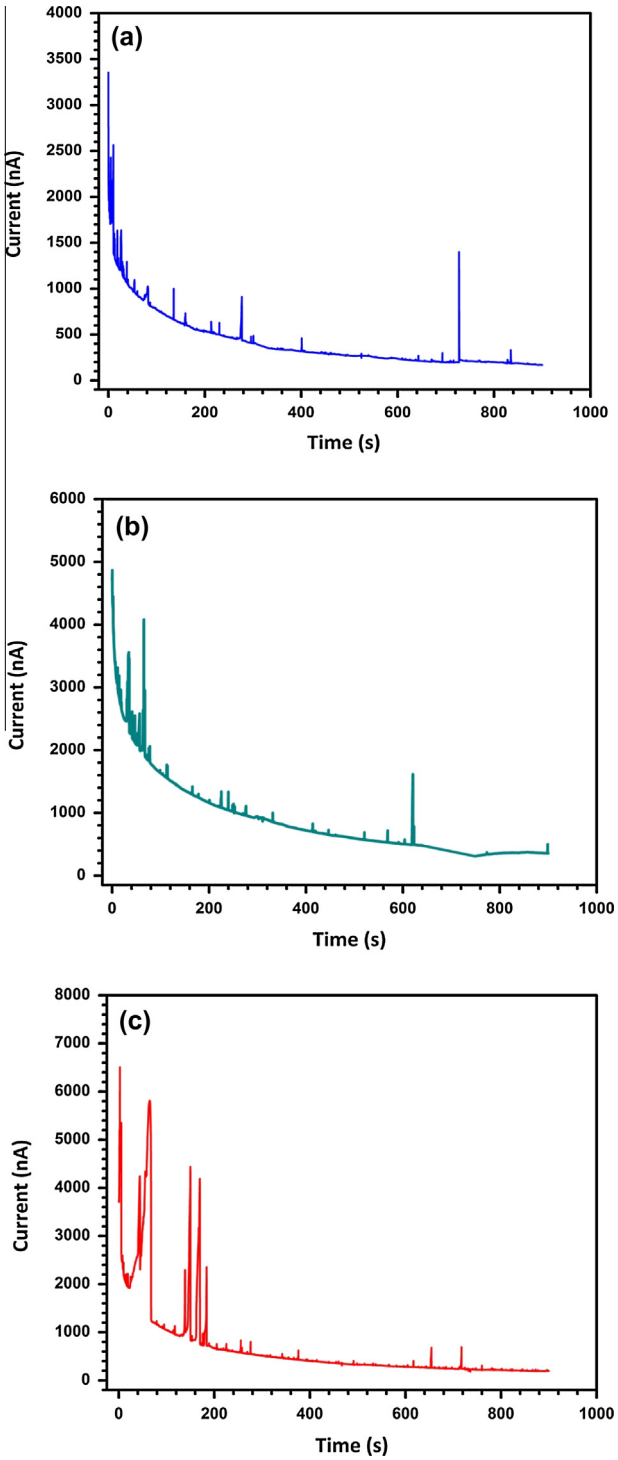


**Fig. 8.** Typical potentiostatic polarisation curves of the sample heat treated at (a) 1050 °C, (b) 1150 °C, and (c) 1250 °C obtained by applying anodic potential of the 80 mV/(SCE) at the temperature of 65 °C.

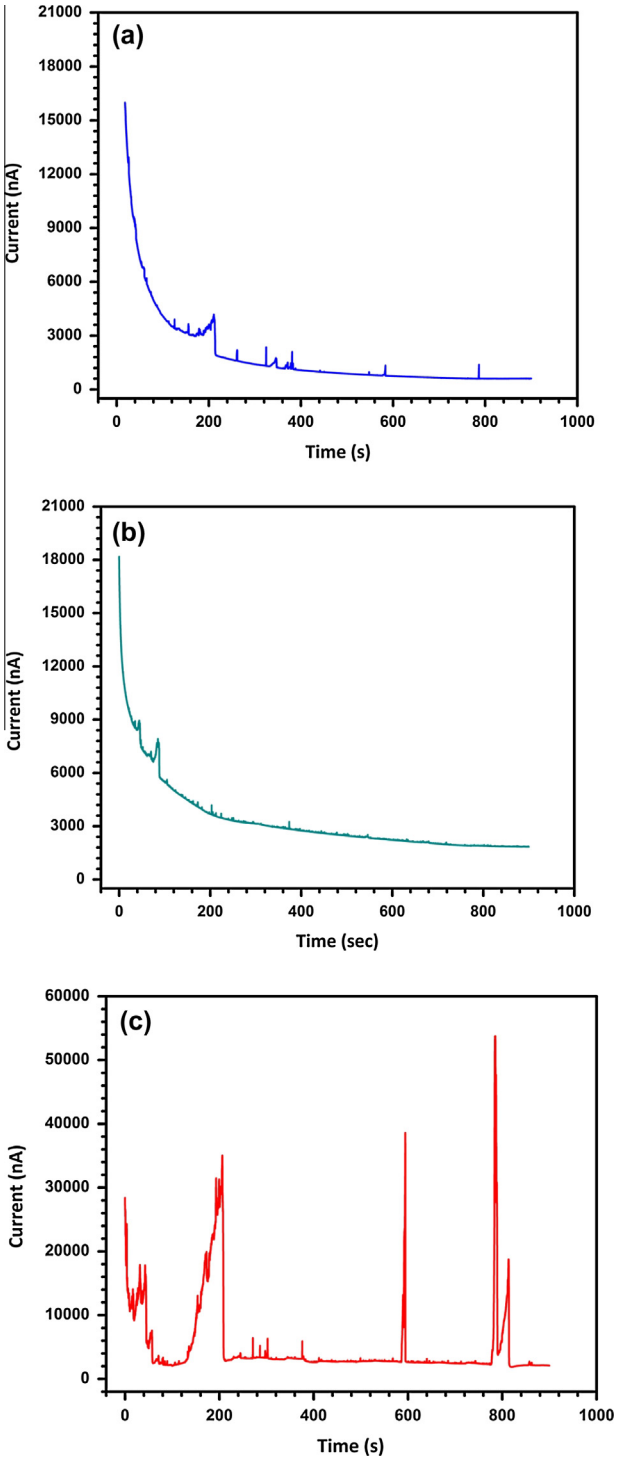


**Fig. 9.** Typical potentiostatic polarisation curves of the sample heat treated at (a) 1050 °C, (b) 1150 °C, and (c) 1250 °C obtained by applying anodic potential of the 800 mV/(SCE) at the temperature of 43 °C.

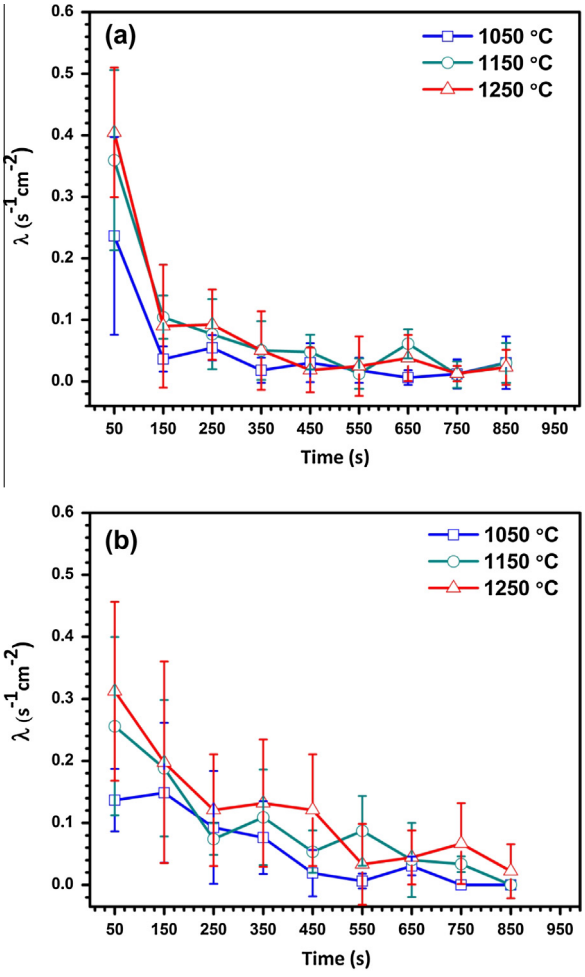


**Fig. 10.** Average of the metastable pits nucleation frequency at (a) 80 mV/(SCE) and 65 °C, (b) 800 mV/(SCE) and 43 °C.

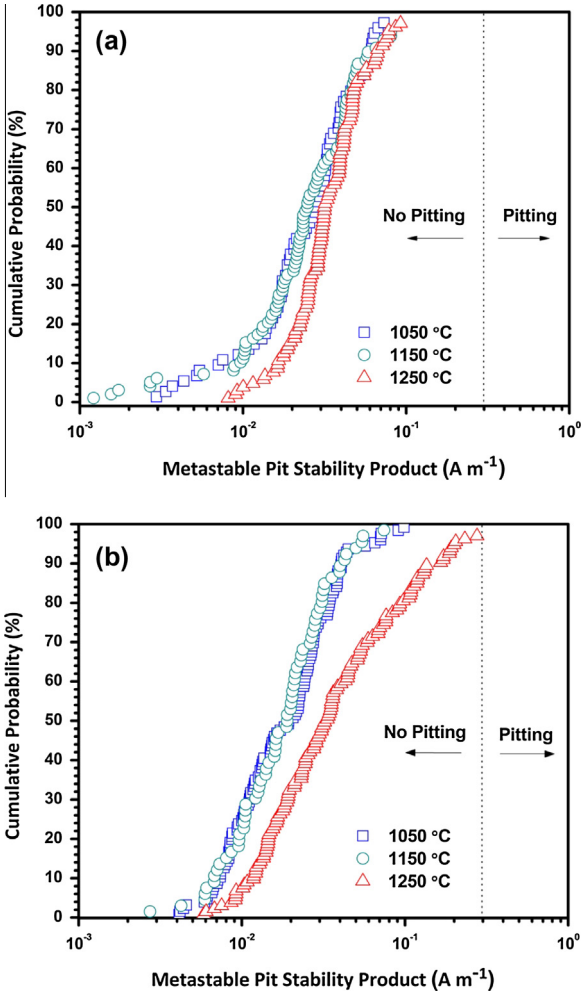


**Fig. 11.** Cumulative distribution of the metastable pits stability product at (a) 80 mV/(SCE) and 65 °C, (b) 800 mV/(SCE) and 43 °C.

the measurements, the sample heat treated at the temperature of 1250 °C has the highest nucleation frequency while the sample heat treated at 1050 °C has the lowest values. Afterward, the nucleation frequency reduces by further increasing in time due to elimination of pit nucleation sites from the electrode surfaces [32,34,52]. It is believed that there is a link between the rate of formation metastable pits ($\lambda$) and the rate of formation stable pit ($\Lambda$) as follows [34]:

$$\Lambda = \lambda \exp(-\mu\tau_C) \tag{3}$$

where $\mu$ ($s^{-1}$) the metastable pit repassivation probability due to rupture of the cover over the pit and $\tau_c$ (s) is the critical duration beyond that a survived metastable pit attains the critical stability product and become stable. In this case, by assuming the $\mu$ and $\tau_c$ as a constant, the sample with higher rate of formation metastable pits ($\lambda$) has the higher rate of formation stable pit ($\Lambda$). Thus, the lower pitting potential and critical pitting temperature value of the sample heat treated at 1250 °C may arise from existence of more preferred sites for pitting initiation on its surface which facilities the formation of the stable pits.

Fig. 11 presents cumulative distribution of the metastable pit stability product for heat treated samples at the anodic potential of 80 and 800 mV/SCE calculated by Eq. (4) [34]:

$$\text{Stability product} = \frac{I_{\text{Peak}}}{2\pi r^2} \times r \tag{4}$$

where $I_{peak}$ is metastable pit peak current (A) and $r$ (m) is the radius of the pit. In this way, by assuming pits as a hemisphere the magnitude of the $r$ is calculated using Faraday equation as follows [32]:

$$\frac{2}{3}\pi r^3 = \frac{ZQ}{nF\rho} \tag{5}$$

where $Z$ (g $mol^{-1}$) is the molar mass of the substance, $Q$ (C) is the total electric charge, $n$ is the valence number of ions of the substance, $F$ is the Faraday constant and $\rho$ (g $m^3$) is the density of the substance. By considering the DSS 2205 as the substance the value of the molar mass, valence number of ions and density equal to 56 g $mol^{-1}$, 2.23 and 7.8 g $cm^{-3}$, respectively.

As it can be seen, by considering the probability values, the samples heat treated at the temperatures of 1050 °C and 1150 °C have the almost same stability product distribution at both anodic potential while the sample heat treated at 1250 °C has higher values. So, the probability of forming stable pits is higher in the samples heat treated at 1250 °C. According to Galvele, the higher potential values provides higher pit current density ($i$) values results in increasing of the stability product ($i.r$) for a defect of given size $r$. So, the probability of forming stable pits form initiation sites with lower depth increases at higher potential. In addition, the importance of the current density in forming stable pits is emphasized by Fig. 12. This figure plots the peak current vs. the calculated radius of the metastable pits at both anodic potentials. As it can be seen, the samples heat treated at 1250 °C have the metastable pits with the almost same radius but with higher

value of the peak current. So, according to Eq. (4) the higher stability product of the metastable pits for the samples heat treated at 1250 °C arise from the higher values of their current. Consequently, presence of the metastable pits with the stability products close to the critical value increases the probability of forming stable pits at the samples heat treated at 1250 °C. Thus, metastable pits measurements also verify that the pitting resistance of the DSS 2205 is reduced with increasing annealing temperature from 1050 °C to 1250 °C.

As it mentioned, the critical pitting temperature and the pitting potential are considered as the main criteria to determine pitting resistance of stainless steels. According to obtained results, both critical pitting temperature and pitting potential of the DSS 2205 are reduced with increasing annealing temperature from 1050 °C to 1250 °C. In this way, microstructure investigations prior to pitting measurement tests expose that Cr and N rich precipitates have been precipitated considerably in ferrite phase at the temperature of 1250 °C. Although, the amounts of this precipitates reduce with decreasing annealing temperature so the samples annealed at the temperature of 1050 °C are free from them. Furthermore, the metastable pits measurements show that the samples heat treated at 1250 °C have the highest nucleation frequency ($\lambda$). In this case, Cr and N rich precipitates and chromium and nitrogen depleted areas around them would be preferred sites for pitting attack [53,54]. As known, the nitrogen and chromium elements have a dominant role on protective properties of the passive layer and growth step of pitting corrosion [55–58]. In this way, reduction of the mentioned elements increases the dissolution rate and facilitates the growth step of the metastable pits. So, it is suggested that the higher values of metastable pit current for the samples heat treated at 1250 °C may come from presence of a lower amounts of chromium and nitrogen elements at ferritic matrix as a result of precipitation the Cr and N rich phases (it can be assumed as chromium nitrides). In addition, according to Eq. (2) the PREN value of the ferrite phase is also reduced by precipitation of these phases. Thus, the ferrite phase is a weaker phase than austenite on the samples heat treated at 1150 °C and 1250 °C and it would be the preferred phase for forming stable pits. It is suggested that precipitation of the Cr and N rich precipitates as secondary phases results in lower pitting corrosion resistance due to consumption of the beneficial passivating elements from ferritic matrix. So, presence of a phase with a lower resistance to pitting corrosion reduces the pitting resistance of the DSS 2205.

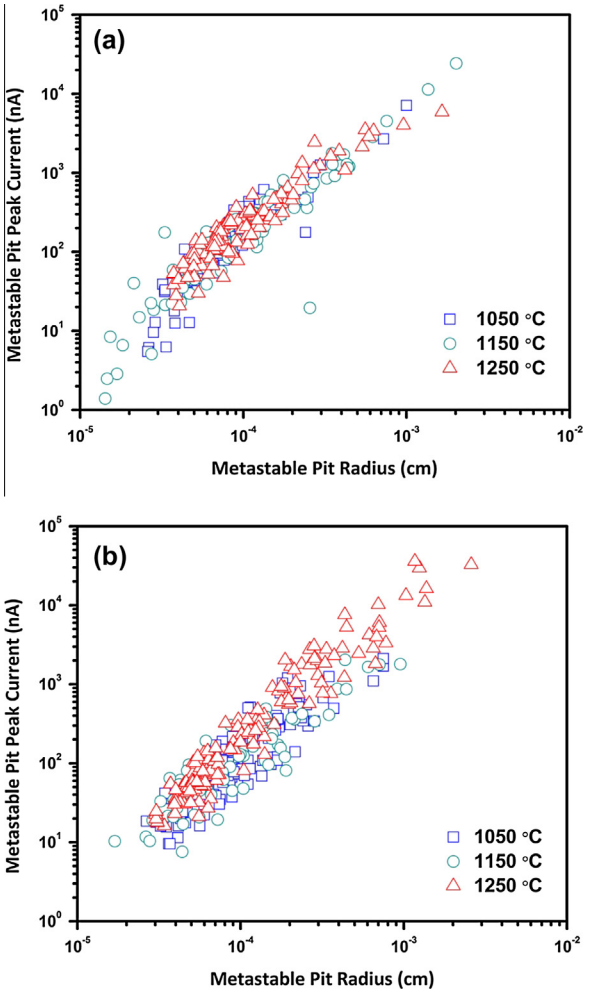


**Fig. 12.** The values of the peak current versus the radius of the corresponding metastable pits at (a) 80 mV/(SCE) and 65 °C, (b) 800 mV/(SCE) and 43 °C.

## 4. Conclusions

In present study, effect of the annealing temperature on pitting corrosion resistance of the DSS 2205 was studied by means of electrochemical techniques and statistical approaches and following results obtained:

1. Microstructure characterization revealed that Cr and N rich phases are precipitated at ferritic matrix after rapid cooling from annealing temperature of 1150 °C and 1250 °C.
2. The critical pitting temperature and pitting potential of the DSS 2205 is reduced by elevating annealing temperature from 1050 °C to 1250 °C.
3. Metastable pitting measurements revealed that metastable pits nucleation frequency and metastable pits stability products are increased with increasing annealing temperature from 1050 °C to 1250 °C.
4. According to microstructure and metastable pits characterization, consumption of the beneficial elements by precipitation of Cr and N rich precipitates such as $Cr_2N$ secondary phases is the main reason of reducing pitting corrosion resistance.

## Acknowledgment

Authors would like to appreciate the financial support from Ferdowsi University of Mashhad provision of laboratory facilities during the period that this research was conducted.

## References

[1] T.P. Hoar, D.C. Mears, G.P. Rothwell, The relationships between anodic passivity, brightening and pitting, Corros. Sci. 5 (1965) 279–289.
[2] C.Y. Chao, L.F. Lin, D.D. Macdonald, A point defect model for anodic passive films: I. Film growth kinetics, J. Electrochem. Soc. 128 (1981) 1187–1194.
[3] H.H. Uhlig, Adsorbed and reaction-product films on metals, J. Electrochem. Soc. 97 (1950) 215C–220C.
[4] N. Sato, A theory for breakdown of anodic oxide films on metals, Electrochim. Acta 16 (1971) 1683–1692.
[5] J.A. Richardson, G.C. Wood, A study of the pitting corrosion of Al byscanning electron microscopy, Corros. Sci. 10 (1970) 313–323.
[6] M. Fregonese, H. Idrissi, H. Mazille, L. Renaud, Y. Cetre, Initiation and propagation steps in pitting corrosion of austenitic stainless steels: monitoring by acoustic emission, Corros. Sci. 43 (2001) 627–641.
[7] E. McCafferty, Sequence of steps in the pitting of aluminum by chloride ions, Corros. Sci. 45 (2003) 1421–1438.
[8] I. Annergren, D. Thierry, F. Zou, Localized electrochemical impedance spectroscopy for studying pitting corrosion on stainless steels, J. Electrochem. Soc. 144 (1997) 1208–1215.
[9] G.S. Eklund, Initiation of pitting at sulfide inclusions in stainless steel, J. Electrochem. Soc. 121 (1974) 467–473.
[10] N. Pessall, C. Liu, Determination of critical pitting potentials of stainless steels in aqueous chloride environments, Electrochim. Acta 16 (1971) 1987–2003.

[11] R. Brigham, E. Tozer, Temperature as a pitting criterion, Corrosion 29 (1973) 33–36.
[12] K. Sasaki, G. Burstein, The generation of surface roughness during slurry erosion–corrosion and its effect on the pitting potential, Corros. Sci. 38 (1996) 2111–2120.
[13] V.M. Salinas-Bravo, R.C. Newman, An alternative method to determine critical pitting temperature of stainless steels in ferric chloride solution, Corros. Sci. 36 (1994) 67–77.
[14] M. Hoseinpoor, M. Momeni, M.H. Moayed, A. Davoodi, EIS assessment of critical pitting temperature of 2205 duplex stainless steel in acidified ferric chloride solution, Corros. Sci. 80 (2014) 197–204.
[15] N. Ebrahimi, M. Momeni, A. Kosari, M. Zakeri, M.H. Moayed, A comparative study of critical pitting temperature (CPT) of stainless steels by electrochemical impedance spectroscopy (EIS), potentiodynamic and potentiostatic techniques, Corros. Sci. 59 (2012) 96–102.
[16] R. Ovarfort, Critical pitting temperature measurements of stainless steels with an improved electrochemical method, Corros. Sci. 29 (1989) 987–993.
[17] T. Shibata, T. Takeyama, Stochastic theory of pitting corrosion, Corrosion 33 (1977) 243–251.
[18] T. Shibata, T. Takeyama, Pitting corrosion as a stochastic process, Nature 260 (1976) 315–316.
[19] T. Shibata, WR Whitney award lecture: statistical and stochastic approaches to localized corrosion, Corrosion 52 (1996) 813–830.
[20] D. Williams, C. Westcott, M. Fleischmann, Stochastic models of pitting corrosion of stainless steels I. Modeling of the initiation and growth of pits at constant potential, J. Electrochem. Soc. 132 (1985) 1796–1804.
[21] D. Williams, C. Westcott, M. Fleischmann, Stochastic models of pitting corrosion of stainless steels II. Measurement and interpretation of data at constant potential, J. Electrochem. Soc. 132 (1985) 1804–1811.
[22] A. Valor, F. Caleyo, L. Alfonso, D. Rivas, J. Hallen, Stochastic modeling of pitting corrosion: a new model for initiation and growth of multiple corrosion pits, Corros. Sci. 49 (2007) 559–579.
[23] T. Shibata, Stochastic studies of passivity breakdown, Corros. Sci. 31 (1990) 413–423.
[24] H. Hong, Application of the stochastic process to pitting corrosion, Corrosion 55 (1999) 10–16.
[25] J. Bastidas, J. Polo, C. Torres, E. Cano, A stochastic approach to study localized corrosion of AISI 304L and AISI 316L stainless steels as a function of potential scan rate, Corrosion 57 (2001) 666–669.
[26] J.W. Provan, E.S. Rodriguez, Part I: Development of a Markov description of pitting corrosion, Corrosion 45 (1989) 178–192.
[27] A.K. Sheikh, J.K. Boah, D.A. Hansen, Statistical modeling of pitting corrosion and pipeline reliability, Corrosion 46 (1990) 190–197.
[28] R. Štefec, F. Franz, A study of the pitting corrosion of cold-worked stainless steel, Corros. Sci. 18 (1978) 161–168.
[29] R.E. Melchers, Statistical characterization of pitting corrosion—Part 1: Data analysis, Corrosion 61 (2005) 655–664.
[30] C. Lemaitre, A. Abdel Moneim, R. Djoudjou, B. Baroux, G. Beranger, A statistical study of the role of molybdenum in the pitting resistance of stainless steels, Corros. Sci. 34 (1993) 1913–1922.
[31] L. Peguet, A. Gaugain, C. Dussart, B. Malki, B. Baroux, Statistical study of the critical pitting temperature of 22-05 duplex stainless steel, Corros. Sci. 60 (2012) 280–283.
[32] D. Nakhaie, M.H. Moayed, Pitting corrosion of cold rolled solution treated 17-4 PH stainless steel, Corros. Sci. 80 (2014) 290–298.
[33] J.R. Galvele, Transport processes and the mechanism of pitting of metals, J. Electrochem. Soc. 123 (1976) 464–474.
[34] P. Pistorius, G. Burstein, Metastable pitting corrosion of stainless steel and the transition to stability, Philos. Trans. R. Soc. Lond., Ser. A 341 (1992) 531–559.
[35] P. Manning, The effect of scan rate on pitting potentials of high performance alloys in acidic chloride solution, Corrosion 36 (1980) 468–474.
[36] K. Ramana, T. Anita, S. Mandal, S. Kaliappan, H. Shaikh, P. Sivaprasad, R. Dayal, H. Khatak, Effect of different environmental parameters on pitting behavior of AISI type 316L stainless steel: experimental studies and neural network modeling, Mater. Des. 30 (2009) 3770–3775.
[37] G. Frankel, Pitting corrosion of metals a review of the critical factors, J. Electrochem. Soc. 145 (1998) 2186–2198.
[38] L. Garfias-Mesias, J. Sykes, C. Tuck, The effect of phase compositions on the pitting corrosion of 25 Cr duplex stainless steel in chloride solutions, Corros. Sci. 38 (1996) 1319–1330.
[39] J. Galvele, J. Lumsden, R. Staehle, Effect of molybdenum on the pitting potential of high purity 18% Cr ferritic stainless steels, J. Electrochem. Soc. 125 (1978) 1204–1208.
[40] S.-H. Jeon, S.-T. Kim, S.-Y. Kim, M.-S. Choi, Y.-S. Park, Effects of solution-annealing temperature on the precipitation of secondary phases and the associated pitting corrosion resistance in hyper duplex stainless steel, Mater. Trans. 54 (2013) 1473–1479.
[41] V. Moura, L. Lima, J. Pardal, A. Kina, R. Corte, S. Tavares, Influence of microstructure on the corrosion resistance of the duplex stainless steel UNS S31803, Mater. Charact. 59 (2008) 1127–1132.
[42] R. Perren, T. Suter, P. Uggowitzer, L. Weber, R. Magdowski, H. Böhni, M. Speidel, Corrosion resistance of super duplex stainless steels in chloride ion containing environments: investigations by means of a new microelectrochemical method: I. Precipitation-free states, Corros. Sci. 43 (2001) 707–726.
[43] R.A. Perren, T. Suter, C. Solenthaler, G. Gullo, P.J. Uggowitzer, H. Böhni, M.O. Speidel, Corrosion resistance of super duplex stainless steels in chloride ion containing environments: investigations by means of a new microelectrochemical method: II. Influence of precipitates, Corros. Sci. 43 (2001) 727–745.
[44] H. Tan, Y. Jiang, B. Deng, T. Sun, J. Xu, J. Li, Effect of annealing temperature on the pitting corrosion resistance of super duplex stainless steel UNS S32750, Mater. Charact. 60 (2009) 1049–1054.
[45] M. Adeli, M. Golozar, K. Raeissi, Pitting corrosion of SAF2205 duplex stainless steel in acetic acid containing bromide and chloride, Electrochem. Commun. 197 (2010) 1404–1416.
[46] B. Deng, Y. Jiang, J. Gao, J. Li, Effect of annealing treatment on microstructure evolution and the associated corrosion behavior of a super-duplex stainless steel, J. Alloys Compd. 493 (2010) 461–464.
[47] Y. Jiang, T. Sun, J. Li, J. Xu, Evaluation of pitting behavior on solution treated duplex stainless steel UNS S31803, J. Mater. Sci. Technol. 30 (2014) 179–183.
[48] Y. Yang, H. Tan, Z. Zhang, Z. Wang, Y. Jiang, L. Jiang, J. Li, Effect of annealing temperature on the pitting corrosion behavior of UNS S82441 duplex stainless steel, Corrosion 69 (2012) 167–173.
[49] A. Ramirez, S. Brandi, J. Lippold, Secondary austenite and chromium nitride precipitation in simulated heat affected zones of duplex stainless steels, Sci. Technol. Weld. Joining 9 (2004) 301–313.
[50] K. Vijayalakshmi, V. Muthupandi, R. Jayachitra, Influence of heat treatment on the microstructure, ultrasonic attenuation and hardness of SAF 2205 duplex stainless steel, Mater. Sci. Eng. A 529 (2011) 447–451.
[51] G.S. Frankel, Pitting corrosion of metals: a review of the critical factors, J. Electrochem. Soc. 145 (1998) 2186–2198.
[52] P. Pistorius, G. Burstein, Aspects of the effects of electrolyte composition on the occurrence of metastable pitting on stainless steel, Corros. Sci. 36 (1994) 525–538.
[53] H. Ha, H. Kwon, Effects of Cr2N on the pitting corrosion of high nitrogen stainless steels, Electrochim. Acta 52 (2007) 2175–2180.
[54] N. Sathirachinda, R. Pettersson, S. Wessman, U. Kivisäkk, J. Pan, Scanning Kelvin probe force microscopy study of chromium nitrides in 2507 super duplex stainless steel—implications and limitations, Electrochim. Acta 56 (2011) 1792–1798.
[55] J. Truman, M. Coleman, K. Pirt, Note on the influence of nitrogen content on the resistance to pitting corrosion of stainless steels, Br. Corros. J. 12 (1977) 236–238.
[56] R. Jargelius-Pettersson, Electrochemical investigation of the influence of nitrogen alloying on pitting corrosion of austenitic stainless steels, Corros. Sci. 41 (1999) 1639–1664.
[57] U. Kamachi Mudali, P. Shankar, S. Ningshen, R. Dayal, H. Khatak, B. Raj, On the pitting corrosion resistance of nitrogen alloyed cold worked austenitic stainless steels, Corros. Sci. 44 (2002) 2183–2198.
[58] J. Horvath, H. Uhlig, Critical potentials for pitting corrosion of Ni, Cr–Ni, Cr–Fe, and related stainless steels, J. Electrochem. Soc. 115 (1968) 791–795.